Inorganic Chemistry

Kinetics of Dissociation of Molecular Oxygen from a Superoxorhodium(III) Complex and Reactivity of a Macrocyclic Rhodium(II) Ion

**Magdalena Furczon, Oleg Pestovsky, and Andreja Bakac***

Ames Laboratory, Iowa State University, Ames, Iowa 50011

Received August 27, 2007

The kinetics of disappearance of the superoxorhodium complex $L^2(H_2O)RhOO^{2+}$ (L^2 = *meso*-hexamethylcyclam) were determined in the presence of several oxidants (H_2O_2, $(NH_3)_5CoBr^{2+}$, and $IrCl_6^{2-}$) in both air-free and air-saturated aqueous solutions. Under air-free conditions, the reaction obeyed first-order kinetics. After the correction for the appropriate stoichiometric factors, the value of the rate constant k_h was the same irrespective of the oxidant, $k_h = 2.18\ (\pm 0.37) \times 10^{-4}\ s^{-1}$ at 25.0 °C in acidic solutions. The disappearance of $L^2(H_2O)RhOO^{2+}$ was slower in the presence of O_2. All the data suggest a sequence of reactions beginning with homolytic dissociation of O_2 from $L^2(H_2O)RhOO^{2+}$, followed by capture of the newly generated $L^2(H_2O)Rh^{2+}$ by added oxidants in competition with O_2. The equilibrium constant for O_2 binding by $L^2(H_2O)Rh^{2+}$ is 10^9-fold greater than that for the cobalt analogue. This difference is attributed to the lower reduction potential of the rhodium complex.

Introduction

Dioxygen activation by transition metal complexes often begins with reversible coordination and partial reduction of O_2, eq 1, where L stands for ligand system, and M for metal.

$$LM^n + O_2 \underset{k_h}{\overset{k_O}{\rightleftharpoons}} LMO_2{}^n \quad K_O \qquad (1)$$
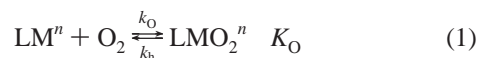
The kinetics of O_2 binding are dominated by the rate of solvent exchange at the metal,[1–5] so that the rate constant k_O for labile metal complexes varies by only a modest factor. The subsequent intramolecular electron transfer to generate $LM^{(n+\delta)}O_2{}^{(\delta-)}$ appears to be fast and, thus, kinetically silent. The reverse of reaction 1, on the other hand, is quite sensitive to the nature of the metal and ligands and has a much greater effect on the equilibrium constant K_O.

The thermodynamics of O_2 binding should, in large part, be determined by the reduction potential of the metal

complex and the steric effects at the M–O_2 site, although other factors such as the solvent, hydrogen bonding, and polar interactions also play a role. The available experimental data qualitatively follow the predicted trend in that the binding is stronger for more electron-rich complexes as judged by their reduction potential or by the electron-donating power and Lewis basicity of the ligands,[2,6–10] although major deviations from the expected behavior have also been reported.[11,12]

Macrocyclic superoxo complexes of cobalt and rhodium persist over a wide range of pH, from acidic to alkaline, which provides an opportunity to examine the role of various parameters on the kinetics and thermodynamics of O_2 binding. This behavior stands in contrast to the superoxo complexes of aqua metal ions, such as $Cr_{aq}OO^{2+}$, which tend to decompose rapidly at pH > 2. Previously, we have determined the kinetics and thermodynamics of O_2 binding

* To whom correspondence should be addressed. E-mail: bakac@ameslab.gov

(1) Falab, S.; Mitchell, P. R. *Adv. Inorg. Bioinorg. Mech.* **1984**, *3*, 311–377.
(2) Bakac, A. *Prog. Inorg. Chem.* **1995**, *43*, 267–351.
(3) Seibig, S.; van Eldik, R. *Inorg. Chem.* **1997**, *36*, 4115–4120.
(4) Korendovych, I. V.; Kryatov, S. V.; Rybak-Akimova, E. V. *Acc. Chem. Res.* **2007**, asap.
(5) Aboelella, N. W.; Kryatov, S. V.; Gherman, B. F.; Brennessel, W. W.; Young, V. G. Jr.; Sarangi, R.; Rybak-Akimova, E. V.; Hodgson, K. O.; Hedman, B.; Solomon, E. I.; Cramer, C. J.; Tolman, W. B. *J. Am. Chem. Soc.* **2004**, *126*, 16896–16911.

(6) Simandi, L. I. *Catalytic Activation of Dioxygen by Metal Complexes*; Kluwer Academic Publishers: Dordercht/Boston/London 1992; Chapter 1.
(7) Momenteau, M.; Reed, C. A. *Chem. Rev.* **1994**, *94*, 659–698.
(8) Collman, J. P.; Gagne, R. R.; Reed, C. A.; Halbert, T. R.; Lang, G.; Robinson, W. T. *J. Am. Chem. Soc.* **1975**, *97*, 1427–1439.
(9) Collman, J. P.; Zhang, X.; Wong, K.; Brauman, J. I. *J. Am. Chem. Soc.* **1994**, *116*, 6245–6251.
(10) Jones, R. D.; Summerville, D. A.; Basolo, F. *Chem. Rev.* **1979**, *79*, 139.
(11) Taube, H. *Prog. Inorg. Chem.* **1986**, *34*, 607–625.
(12) Wong, C.-L.; Switzer, J. A.; Balakrishnan, K. P.; Endicott, J. F. *J. Am. Chem. Soc.* **1980**, *102*, 5511–5518.

in $L^2(H_2O)CoOO^{2+}$ ($L^2 = meso$-Me$_6$-[14]aneN$_4$) in acidic aqueous solutions.[2] The binding ($K = 300$ M^{-1}) is much weaker than that in the related complex with L^1 ($L^1 = $ [14]-aneN$_4$), $K = 1.9 \times 10^5$ M^{-1}. The difference between the two can be explained by a combination of smaller steric crowding in $L^1(H_2O)CoOO^{2+}$ and by somewhat lower reduction potential of $L^1Co(H_2O)_2^{3+/2+}$ ($E_{1/2} = 0.44$ V)[13] than of the L^2 analogue, $E_{1/2} = 0.49$[13] or 0.59 V[14] in 0.10 M HClO$_4$. We have now obtained data for a rhodium complex $L^2(H_2O)RhOO^{2+}$ and examined directly the effect of the metal in an otherwise identical ligand and solvent environment. Previous work has already established the greater stability of the rhodium complex which has allowed us to determine its crystal structure by X-ray diffraction.[15]

$L^2(H_2O)RhOO^{2+}$ $L^1(H_2O)CoOO^{2+}$
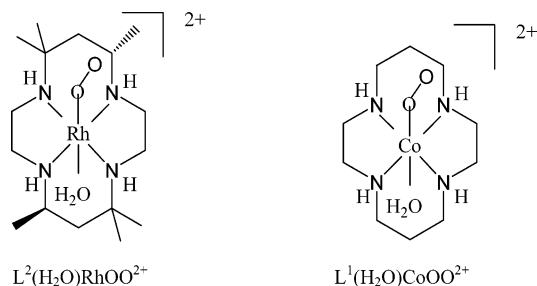
Experimental Section

The hydride $[L^2(H_2O)RhH](CF_3SO_3)_2$ was prepared as previously described.[16] Dilute solutions of $L^2(H_2O)Rh^{2+}$ (≤ 1 mM) were generated photochemically[17] and injected into oxygen-saturated 0.5 mM aqueous HClO$_4$ to prepare solutions of $L^2(H_2O)RhOO^{2+}$ (0.02−0.05 mM). For air-free work, these solutions were made alkaline with NaOH (final concentration 2 mM), deaerated with a stream of argon for 30−40 min, and reacidified with HClO$_4$, typically to [H$^+$] = 0.10 M. In laser flash photolysis experiments, micromolar concentrations of $L^2(H_2O)Rh^{2+}$ were generated from $L^2(H_2O)RhOO^{2+}$ by a 355 nm flash from a Nd/YAG laser.

UV−vis spectral and kinetic measurements utilized a Shimadzu 3101 PC spectrophotometer at a constant temperature of 25.0 ± 0.2 °C. Laser flash photolysis experiments were done with the LKS 50 Applied Photophysics laser flash photolysis instrument.[18] In-house distilled water was further purified by passage through a Barnstead EASYpure III system.
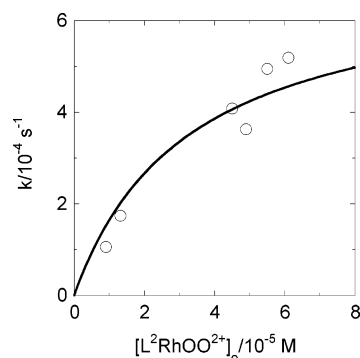
Depending on the oxidant, the homolysis rate constant was determined either from the initial rates or by fitting the kinetic curves to a first-order rate expression.

Results

The complex $L^2(H_2O)RhOO^{2+}$ persists for many hours at room temperature in acidic O$_2$-saturated aqueous solutions but decomposes readily if O$_2$ is removed. These observations are consistent with the reaction in eq 2 whereby the removal of O$_2$ pulls the equilibrium to the right.

$$L^2(H_2O)RhOO^{2+} \underset{k_O}{\overset{k_h}{\rightleftharpoons}} L^2(H_2O)Rh^{2+} + O_2 \quad K_h \quad (2)$$
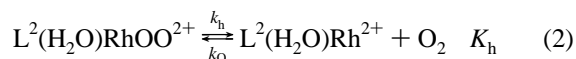
In the absence of scavengers, the rate constant for the disappearance of $L^2(H_2O)RhOO^{2+}$ in carefully deaerated,

(13) Heckman, R. A.; Espenson, J. H. *Inorg. Chem.* **1979**, *18*, 38−43.
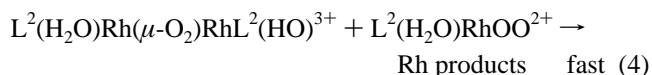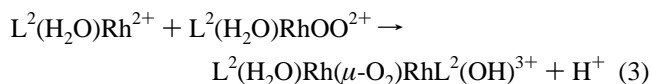(14) Liteplo, M. P.; Endicott, J. F. *Inorg. Chem.* **1971**, *10*, 1420−1430.

Figure 1. Plot of the rate constant for the decay of $L^2(H_2O)RhOO^{2+}$ as a function of its concentration. The line is a fit to eq 5 using $k_h = 2.3 \times 10^{-4}$ s^{-1}, $k_O = 8 \times 10^7$ M^{-1} s^{-1}, and O$_2$ = 1 μM.

argon-saturated solutions was determined from initial rates. This approach was adopted to avoid complications caused by the steady increase in O$_2$ concentration and the growing importance of the reverse step as the reaction progresses.

No External Substrates Added. The molar absorption coefficient of $L^2(H_2O)RhOO^{2+}$ at 272 nm, $\epsilon_{RhOO} = 1.0 \times 10^4$ M^{-1} cm^{-1}, was known from our earlier work,[19] and that for the product was determined after the reaction had been allowed to go to completion, $\epsilon_{prod} = 1.3 \times 10^3$ M^{-1} cm^{-1}. The difference, $\Delta\epsilon_{272}$, was used to convert the initial absorbance changes into initial rates which were in turn divided by $[L^2(H_2O)RhOO^{2+}]_0$ to obtain the rate constants k_{obs}. These apparent first-order rate constants increased with increasing concentrations of the superoxo complex, and visually appeared to saturate around $(6-7) \times 10^{-4}$ s^{-1}, Figure 1. Even though the scatter is somewhat large, owing to the complex experimental protocol (see Experimental Section) and small absorbance changes used in the determination of initial rates, the data are clearly consistent with the mechanism in eqs 2−4 and the associated rate law in eq 5, as discussed below.

The initial product of reaction 4 may be the μ-superoxo dirhodium(III) complex, but no intense absorption expected[16] for such a complex at ∼360 nm was observed, either because it was not formed or because it had decomposed rapidly to a more stable Rh(III) product(s). Independent spectrophotometric titration with $L^2(H_2O)Rh^{2+}$ at 272 nm provided the stoichiometric ratio for reactions 3−4, $[L^2(H_2O)RhOO^{2+}]/[L^2(H_2O)Rh^{2+}] = 2.0 \pm 0.2$.

$$L^2(H_2O)Rh^{2+} + L^2(H_2O)RhOO^{2+} \rightarrow$$
$$L^2(H_2O)Rh(\mu\text{-}O_2)RhL^2(OH)^{3+} + H^+ \quad (3)$$

$$L^2(H_2O)Rh(\mu\text{-}O_2)RhL^2(HO)^{3+} + L^2(H_2O)RhOO^{2+} \rightarrow$$
$$\text{Rh products} \quad \text{fast} \quad (4)$$

(15) Bakac, A.; Guzei, I. A. *Inorg. Chem.* **2000**, *39*, 736−740.
(16) Bakac, A. *J. Am. Chem. Soc.* **1997**, *119*, 10726−10731.
(17) Bakac, A. *Dalton Trans.* **2007**, 1589−1596.
(18) Huston, P.; Espenson, J. H.; Bakac, A. *J. Am. Chem. Soc.* **1992**, *114*, 9510−9516.
(19) Pestovsky, O.; Bakac, A. *J. Am. Chem. Soc.* **2002**, *124*, 1698−1703.

$$-d[[L^2RhOO^{2+}]/dt =$$

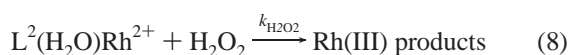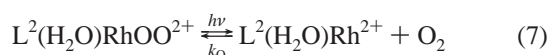$$3k_h[L^2RhOO^{2+}] \frac{k_3[L^2RhOO^{2+}]}{k_3[L^2RhOO^{2+}] + k_O[O_2]} \quad (5)$$

In the proposed mechanism, the kinetic effect of $[L^2(H_2O)\text{-}RhOO^{2+}]$ in Figure 1 is explained by competition between $L^2(H_2O)RhOO^{2+}$ and O_2 for $L^2(H_2O)Rh^{2+}$. The observed rate constant reaches a plateau only when $[L^2(H_2O)RhOO^{2+}]$ becomes sufficiently large to make reaction 3 much faster than reaction -2. At this point, the second term in the denominator of eq 5 becomes negligibly small and the expression reduces to eq 6.

$$-d[[L^2RhOO^{2+}]/dt = 3k_h[L^2RhOO^{2+}] \quad (6)$$

The data in Figure 1 could not be fitted to eq 5 to obtain a precise value of k_h because eq 5 contains too many unknowns, i.e., k_h, k_3, and $[O_2]$. Small concentrations of O_2 are always present in our solutions as trace impurity and also as a product of reaction 2. Instead, we used the data in Figure 2 to confirm the qualitative agreement with eq 5 and to obtain an estimate for k_3. To this purpose, we fixed k_h at the value obtained in the presence of various scavengers for $L^2(H_2O)Rh^{2+}$ ($k_h = 2.2 \times 10^{-4}$ s^{-1}, see below) and estimated the concentration of O_2 as 10 μM $\geq [O_2] \geq 1$ μM. The fit, shown in Figure 1, yielded 3×10^7 M^{-1} s^{-1} $\geq k_3 \geq 3 \times 10^6$ M^{-1} s^{-1}.

Additional kinetic experiments utilized several externally added scavengers for $L^2(H_2O)Rh^{2+}$, namely H_2O_2, $IrCl_6^{2-}$, and $Co(NH_3)_5Br^{2+}$. For all of these, the kinetics of the $L^2(H_2O)Rh^{2+}$/scavenger reactions had to be determined first, as described below.

$L^2(H_2O)Rh^{2+}$/H_2O_2 Reaction. The kinetics were determined by laser flash photolysis of $L^2(H_2O)RhOO^{2+}$ in the presence of H_2O_2 and air as competitors for $L^2(H_2O)Rh^{2+}$, eqs 7−8.

$$L^2(H_2O)RhOO^{2+} \underset{k_O}{\overset{h\nu}{\rightleftharpoons}} L^2(H_2O)Rh^{2+} + O_2 \quad (7)$$

$$L^2(H_2O)Rh^{2+} + H_2O_2 \xrightarrow{k_{H2O2}} \text{Rh(III) products} \quad (8)$$

The rate constants obtained from the signals at 272 nm are plotted against $[H_2O_2]$ in Figure 2. The data obey the rate law in eq 9.

$$-d[L^2(H_2O)Rh^{2+}]/dt =$$

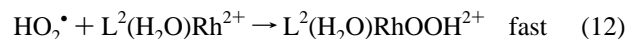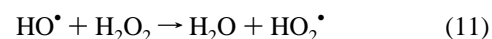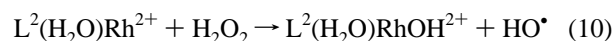$$(k_O[O_2] + k_{H2O2}[H_2O_2])[L^2(H_2O)Rh^{2+}] \quad (9)$$

The intercept in Figure 2 was determined independently in the absence of H_2O_2. The value, $(1.99 \pm 0.10) \times 10^4$ s^{-1}, is acceptably close to that calculated (2.13×10^4 s^{-1}) from the known k_O (8.2×10^7 M^{-1} s^{-1})[20] and the concentration of O_2 in air-saturated solutions (2.6×10^{-4} M). The slope yielded $k_{H2O2} = (7.34 \pm 0.85) \times 10^5$ M^{-1} s^{-1}.

A plausible scheme for the $L^2(H_2O)Rh^{2+}$/H_2O_2 reaction is shown in eqs 10−12. The HO$^{\bullet}$ radicals generated in eq
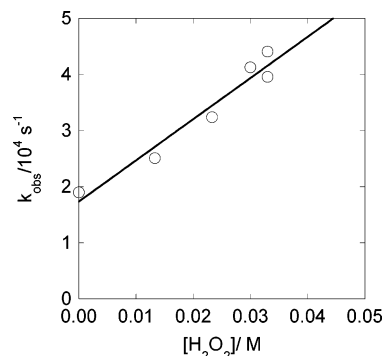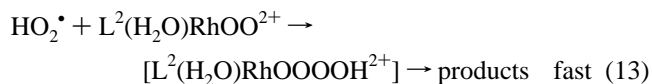

Figure 2. Plot of the rate constant against the concentration of H_2O_2 for the reaction with $L^2(H_2O)Rh^{2+}$ generated by laser flash photolysis of $L^2(H_2O)RhOO^{2+}$.

10 react with H_2O_2 ($k_{11} = 5 \times 10^7$ M^{-1} s^{-1})[21] to generate HO$_2^{\bullet}$ radicals which should be scavenged by $L^2(H_2O)Rh^{2+}$ in a fast follow-up step. According to this mechanism, the observed rate constant k_{H2O2} contains a stoichiometric factor of 2, i.e., $k_{10} = 0.5k_{H2O2} = (3.67 \pm 0.42) \times 10^5$ M^{-1} s^{-1}.

$$L^2(H_2O)Rh^{2+} + H_2O_2 \rightarrow L^2(H_2O)RhOH^{2+} + HO^{\bullet} \quad (10)$$

$$HO^{\bullet} + H_2O_2 \rightarrow H_2O + HO_2^{\bullet} \quad (11)$$

$$HO_2^{\bullet} + L^2(H_2O)Rh^{2+} \rightarrow L^2(H_2O)RhOOH^{2+} \quad \text{fast} \quad (12)$$

In thermal homolysis experiments, the steady-state concentration of $L^2(H_2O)Rh^{2+}$ is low, and it is highly unlikely that reaction 12 would be important. The most reasonable fate of HO$_2^{\bullet}$ under those conditions is shown in eq 13, similar to the reactions of other radicals (RC(O)OO$^{\bullet}$, $^{\bullet}$NO, Br$_2^{\bullet-}$, etc.) with superoxometal complexes.[20]

$$HO_2^{\bullet} + L^2(H_2O)RhOO^{2+} \rightarrow$$

$$[L^2(H_2O)RhOOOOH^{2+}] \rightarrow \text{products} \quad \text{fast} \quad (13)$$

$L^2(H_2O)Rh^{2+}$/$IrCl_6^{2-}$ Reaction. The kinetics were determined by laser flash photolysis of air-free 0.10 M HClO$_4$ containing $L^2(H_2O)RhOO^{2+}$ (33−35 μM) and $IrCl_6^{2-}$ (26−122 μM). The loss of $IrCl_6^{2-}$ in reaction 14 was monitored at 487 nm, where $IrCl_6^{2-}$ exhibits a maximum with $\epsilon = 3920$ M^{-1} cm^{-1}.[22]

$$L^2(H_2O)Rh^{2+} + IrCl_6^{2-} \xrightarrow{H_2O} L^2(H_2O)_2Rh^{3+} + IrCl_6^{3-} \quad k_{IrCl} \quad (14)$$
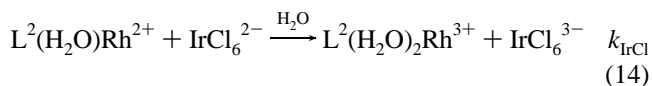
The pseudo-first-order rate constants obtained from the exponential kinetic traces are directly proportional to the concentration of $IrCl_6^{2-}$, Figure 3. The slope of the line gives $k_{IrCl} = (5.4 \pm 0.2) \times 10^9$ M^{-1} s^{-1}.

Products of reaction 14 have not been determined. The reaction is written as an outer-sphere process, but inner-sphere electron transfer to yield $L^2(H_2O)_2RhCl^{2+}$ + Ir(H$_2$O)Cl$_5^{3-}$ is also possible. At the low concentrations used

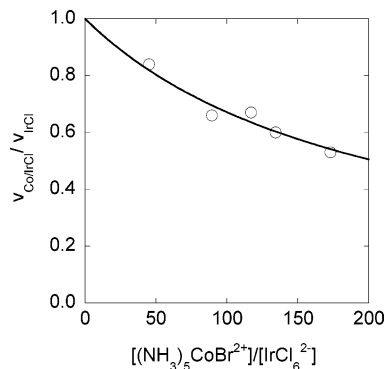(20) Bakac, A. *Adv. Inorg. Chem.* **2004**, *55*, 1−59.

(21) Buxton, G. V.; Greenstock, C. L.; Helman, W. P.; Ross, A. B. *J. Phys. Chem. Ref. Data* **1988**, *17*, 513−886.
(22) Hurwitz, P.; Kustin, K. *Inorg. Chem.* **1964**, *3*, 823−826.
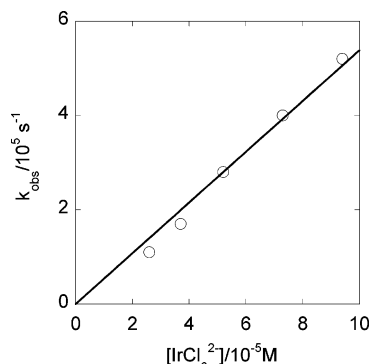
Figure 3. Plot of k_{obs} against the concentration of $IrCl_6^{2-}$ for the reaction with $L^2(H_2O)Rh^{2+}$ in 0.10 M $HClO_4$.

Figure 4. Plot of the rate ratio as a function of the concentration ratio, $[(NH_3)_5CoBr^{2+}]/[IrCl_6^{2-}]$. The line is the fit to eq 16.

in these experiments, the spectra of the products[23-25] are too weak for unambiguous identification.

$L^2(H_2O)Rh^{2+}/(NH_3)_5CoBr^{2+}$ Reaction. The rate constant was determined in competition experiments with $IrCl_6^{2-}$. $L^2(H_2O)Rh^{2+}$ was generated by thermal homolysis of $L^2(H_2O)RhOO^{2+}$. The initial rates of disappearance of $IrCl_6^{2-}$ (34−47 μM) were first determined in solutions of $L^2(H_2O)RhOO^{2+}$ (20−30 μM). When $Co(NH_3)_5Br^{2+}$ (2.3−6.4 mM) was added, the rates decreased, as expected if $Co(NH_3)_5Br^{2+}$ and $IrCl_6^{2-}$ competed for $L^2(H_2O)Rh^{2+}$, eqs 2, 14, and 15.

$$L^2(H_2O)Rh^{2+} + Co(NH_3)_5Br^{2+} (+ 5H^+) \rightarrow$$
$$L^2(H_2O)Rh^{3+} + Co_{aq}^{2+} + 5NH_4^+ + Br^- \quad k_{Co} \quad (15)$$
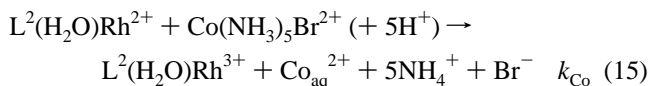
The ratios of the initial rates in the presence ($v_{Co/IrCl}$) and absence (v_{IrCl}) of the cobalt complex are plotted against the ratio $[Co(NH_3)_5Br^{2+}]/[IrCl_6^{2-}]$ in Figure 4. The fit to eq 16 yielded the ratio $k_{Co}/k_{IrCl} = (4.9 \pm 0.3) \times 10^{-3}$, and thus $k_{Co} = (2.6 \pm 0.3) \times 10^7$ M^{-1} s^{-1}.

$$\frac{v_{Co/IrCl}}{v_{IrCl}} = \frac{k_{IrCl}[IrCl_6^{2-}]}{k_{IrCl}[IrCl_6^{2-}] + k_{Co}[(NH_3)_5CoBr^{2+}]} = \frac{1}{1 + \dfrac{k_{Co}[(NH_3)_5CoBr^{2+}]}{k_{IrCl}[IrCl_6^{2-}]}} \quad (16)$$

(23) Sykes, A. G.; Thorneley, R. N. F. *J. Chem. Soc. A* **1970**, 232−238.

Table 1. Summary of Kinetic Data for Reactions of $L^2(H_2O)Rh^{2+}$ with Oxidants

| oxidant	k/M^{-1} s^{-1}
H_2O_2	$(3.67 \pm 0.42) \times 10^5$
$(NH_3)_5CoBr^{2+}$	$(2.6 \pm 0.3) \times 10^7$
$IrCl_6^{2-}$	$(5.38 \pm 0.16) \times 10^9$

A summary of all the kinetic data for the oxidation of $L^2(H_2O)Rh^{2+}$ obtained in this work is given in Table 1.

In an attempt to determine the reduction potential for the $L^2(H_2O)Rh^{3+/2+}$ couple, we briefly examined the reactions of $L^2(H_2O)Rh^{2+}$ with Cu_{aq}^{2+} ($E^0 = 0.159$ V)[26] and $Ru(NH_3)_6^{3+}$ ($E^0 = 0.10$ V). The oxidation of $L^2(H_2O)Rh^{2+}$ (0.1−0.3 mM), monitored at 245 nm, with several equivalents of Cu_{aq}^{2+} in 0.10 M $HClO_4$ proceeded to completion, which places the equilibrium constant for the $L^2(H_2O)Rh^{2+}/Cu_{aq}^{2+}$ reaction, K_{RhCu}, at ≥ 1, and the $L^2(H_2O)Rh^{3+/2+}$ potential at ≤ 0.159 V. When mixtures of Cu_{aq}^+ and Cu_{aq}^{2+} were used, the absorbance changes were smaller and the reactions somewhat faster, indicating that equilibrium had been reached at less than 100% completion. Owing to the tendency of Cu_{aq}^+ to disproportionate, only limiting amounts (≤ 1 mM) could be added, which limited the precision of the equilibrium data. We obtained $1 \leq K_{RhCu} \leq 10$, and $E(L^2(H_2O)Rh^{3+/2+}) = 0.13 \pm 0.03$ V. No reaction was observed between $L^2(H_2O)Rh^{2+}$ and $Ru(NH_3)_6^{3+}$, apparently for kinetic reasons.

Kinetics of Rh−O₂ Homolysis. H₂O₂ as Scavenger. Experiments were conducted in both argon-saturated and air-saturated solutions. The exponential kinetic traces yielded first-order rate constants shown in Figures 5 and 6. In the absence of oxygen in 0.10 M $HClO_4$, the plot of k_{obs} against $[H_2O_2]$ is linear with a slope of $(2.14 \pm 0.33) \times 10^{-3}$ M^{-1} s^{-1} and an intercept of $(4.60 \pm 0.07) \times 10^{-4}$ s^{-1}, Figure 5.

The slope indicates a direct reaction between H_2O_2 and $L^2(H_2O)RhOO^{2+}$, which probably takes place by hydrogen atom abstraction from H_2O_2, eq 17 followed by eq 13. The observed slope thus corresponds to $2k_{17}$. This chemistry is closely related to the reaction of this and other superoxometal complexes with metal hydroperoxides. As expected, free H_2O_2 reacts several orders of magnitude more slowly than metal hydroperoxides.[27]

$$H_2O_2 + L^2(H_2O)RhOO^{2+} \rightarrow L^2(H_2O)RhOOH^{2+} + HO_2^\bullet \quad (17)$$
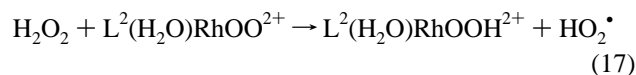
The most reasonable mechanism for the H_2O_2-independent path is the homolysis (eq 2) followed by the chemistry in eqs 10, 11, and 13, so that the intercept in Figure 5 equals $2k_h$, i.e., $k_h = (2.30 \pm 0.03) \times 10^{-4}$ s^{-1}.
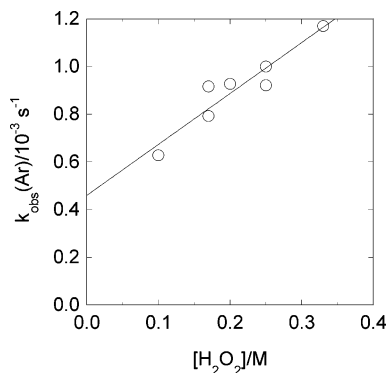
The disappearance of $L^2(H_2O)RhOO^{2+}$ was again slower in air-saturated solutions, Figure 6, as one would expect on the basis of the retarding effect of O_2 on reaction 2. The same mechanism applies as in air-free solutions, i.e., the

(24) Bounsall, E. J.; Koprich, S. R. *Can. J. Chem.* **1970**, *48*, 1481−1491.
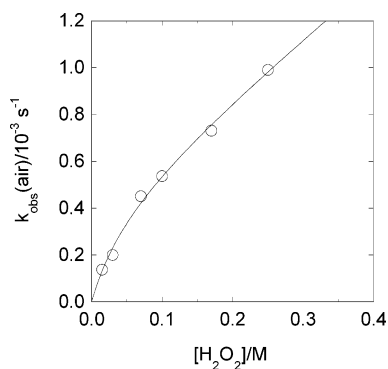(25) Curtis, N. F.; Cook, D. F. *J. Chem. Soc. Dalton Trans.* **1972**, 691−697.
(26) Bard, A. J.; Parsons, R.; Jordan, J. *Standard Potentials in Aqueous Solution*; Marcel Dekker: New York, Basel, 1985.
(27) Vasbinder, M.; Bakac, A. *Inorg. Chem.* **2007**, *46*, 2921−2928.

Figure 5. Plot of the observed rate constant for the disappearance of $L^2(H_2O)RhOO^{2+}$ against the concentration of H_2O_2 in air-free 0.10 M $HClO_4$.

Figure 6. Plot of the observed rate constant against the concentration of H_2O_2 for the homolysis of $L^2(H_2O)RhOO^{2+}$ in air-saturated solutions. The line is the fit to eq 18.

Table 2. Summary of Kinetic Data for k_h under Air-Free Conditions at 25.0 °C and pH 1

scavenger	$k_h/10^{-4}\,s^{-1}$
$L^2(H_2O)RhOO^{2+}$	2–3
H_2O_2	2.30 ± 0.35
$H_2O_2{}^a$	2.26 ± 0.24
$(NH_3)_5CoBr^{2+}$	1.65 ± 0.05
$IrCl_6{}^{2-}$	2.50 ± 0.20
average	2.18 ± 0.37

^{a} In air-saturated solutions.

direct $L^2(H_2O)RhOO^{2+}/H_2O_2$ reaction takes place in parallel with the homolysis scheme of eqs 2, 10, 11, and 13. The rate law of eq 18 is applicable to both sets of conditions, but the term $k_O[O_2]$ in the denominator becomes negligible under argon which simplifies the expression to that observed, i.e., $k_{obs} = 2k_h + 2k_{17}$. The treatment of the data obtained in air-saturated solutions, on the other hand, requires the use of the complete expression in eq 18.

With k_8 and k_O fixed at their known values, Table 1, the fit in Figure 6 yielded $k_{17} = (1.23 \pm 0.12) \times 10^{-3}\,M^{-1}\,s^{-1}$ and $2k_h = (2.26 \pm 0.26) \times 10^{-4}\,s^{-1}$, both in good agreement with the values obtained under argon. All the homolysis data are summarized in Table 2.

$$k_{obs} = 2k_{17}[H_2O_2] + \frac{2k_h k_8[H_2O_2]}{k_8[H_2O_2] + k_O[O_2]} \qquad (18)$$

$IrCl_6{}^{2-}$ as Scavenger. From the initial rates of disappearance of $IrCl_6{}^{2-}$ (0.126–0.378 mM) in the presence of 0.034

Table 3. Kinetic Data for O_2 Binding and Release by Some Mononuclear Transition Metal Complexes in Aqueous Solutions^a

LM^n	$k_O/M^{-1}\,s^{-1}$	k_h/s^{-1}	K_O/M^{-1}
$L^1(H_2O)_2Co^{2+}$	1.2×10^7	63	1.9×10^5
$L^2(H_2O)_2Co^{2+}$	5.0×10^6	1.66×10^4	3.0×10^2
$L^2(Cl)(H_2O)Co^+$	1.8×10^6	3.21×10^3	5.6×10^2
$L^2(SCN)(H_2O)Co^+$	7.3×10^6	1.77×10^1	4.1×10^5
$L^2(OH)(H_2O)Co^+$	8.9×10^5	2.1×10^{-2}	4.2×10^7
$L^2(H_2O)Rh^{2+}$	8.2×10^7	2.18×10^{-4}	3.7×10^{11}
$Cr(H_2O)_6{}^{2+}$	1.6×10^8	2.5×10^{-4}	6.4×10^{11}

^{a} Data from this work and ref 2 and 20. L^1 = cyclam, L^2 = Me$_6$-cyclam.

mM $L^2(H_2O)RhOO^{2+}$, the rate constant $k_h = (2.50 \pm 0.20) \times 10^{-4}\,s^{-1}$ was obtained.

$(NH_3)_5CoBr^{2+}$ as Scavenger. $(NH_3)_5CoBr^{2+}$ absorbs intensely in the UV, which has limited the concentrations of this scavenger to $\leq 3 \times 10^{-4}$ M and required the use of initial rates. The measurements were carried out at 280 nm, where the calculated difference in molar absorptivities between the reactants and products was determined to be $1.07 \times 10^4\,M^{-1}\,cm^{-1}$. Two experiments with $[L^2(H_2O)\text{-}RhOO^{2+}]_0 = 0.050$ mM, and $(NH_3)_5CoBr^{2+} = 0.10$ mM and 0.28 mM yielded $k_h = 1.7 \times 10^{-4}$ and $1.6 \times 10^{-4}\,s^{-1}$, respectively. These values are somewhat lower than those obtained by other scavengers. At the concentrations used, $(NH_3)_5CoBr^{2+}$ should be able to scavenge $>90\%$ of $L^2(H_2O)\text{-}Rh^{2+}$ in competition with O_2 even if the latter is present at three times higher concentrations than the expected 2 μM in the initial stages of the reaction. Most likely, the small k_h is the result of the uncertainty in $\Delta\epsilon$ at 280 nm, a wavelength that lies on a steep, rising portion of the spectra of both reagents.

Discussion

The complex $L^2(H_2O)Rh^{2+}$ binds O_2 about 10^9 times more strongly than $L^2(H_2O)_2Co^{2+}$ does. In fact, as shown in Table 3, the binding constant K_O is comparable to that of the strongly reducing and sterically unencumbered Cr_{aq}^{2+}. As is usually the case, the kinetics of O_2 binding to the three reductants are not too different. The equilibrium constants are determined mainly by the dissociation kinetics, i.e., by k_h.

Quantitative kinetic data are not available for the homolysis of the superoxorhodium complex in alkaline solutions, but its stability is greatly enhanced under such conditions, as evidenced by our ability to handle such solutions at pH ≥ 9 in the absence of air for extended periods of time without observable loss of the superoxide. Clearly, O_2 binding under such conditions is again much stronger for the rhodium than for the cobalt analogue, $L^2(OH)CoOO^+$, which has $K_O = 4.2 \times 10^7\,M^{-1}$ and $k_h = 0.021\,s^{-1}$, so that even alkaline solutions of the superoxocobalt decay readily upon purging with an inert gas.

The reduction potentials for the two $L^2(H_2O)M^{3+/2+}$ complexes are around 0.13 V (M = Rh), estimated in this work, and 0.49[13] or 0.59 V[14] (M = Co). This difference in potentials for the two couples translates into a 10^6–10^8-fold greater equilibrium constant for the reduction of O_2 by $L^2(H_2O)Rh^{2+}$. Thus, a great portion of the observed 10^9-fold

difference in the stability of the two superoxo complexes, Table 3, is accounted for by the difference in reduction potentials for the $L^2(H_2O)M^{3+/2+}$ complexes.

As noted earlier,[11,12,28] the stability constants of $L(H_2O)$-$CoOO^{2+}$ ($L = L^1$ and L^2) are unusually large in the superoxocobalt(III) formalism; the binding of superoxide, a weak base, to cobalt(III) appears to be stronger than the binding of hydroxide. The extra stability was suggested to come from charge transfer interactions in the complex.[11] Apparently, the same is true for $L^2(H_2O)RhOO^{2+}$, with K_O approaching that of the much more reducing $Cr(H_2O)_6^{2+}$.

From the experimentalist's point of view, Rh(II) complexes are more difficult to generate than some other reduced metal complexes[17] which can be often obtained by Zn/Hg reduction of a higher oxidation state of the metal. When applied to Rh(III), this approach typically does not produce Rh(II) but instead generates the hydrides. The more common routes to Rh(II) are thus based on photochemical cleavage of the Rh$-$H bond.[17] As shown in this work, thermal homolysis of the superoxo complex, eq 2, is also a good source of $L^2(H_2O)Rh^{2+}$ for kinetic and mechanistic work. In some situations, such as competition experiments, this method is superior to photohomolysis in photochemical reactors or by flash methods. Further work on the reactivity of Rh(II) complexes is in progress in our laboratories.

(28) Bakac, A.; Espenson, J. H. *J. Am. Chem. Soc.* **1990**, *112*, 2273−2278.

IC701686G